Journal of Statistical Physics, Vol. 90, Nos. 1/2, 1998

Stochastic Calculus: Application to Dynamic Bifurcations and Threshold Crossings

Kalvis M. Jansons[1] and G. D. Lythe[2]

Received July 9, 1996; final July 7, 1997

For the dynamic pitchfork bifurcation in the presence of white noise, the statistics of the last time at zero are calculated as a function of the noise level ε and the rate of change of the parameter μ. The threshold crossing problem used, for example, to model the firing of a single cortical neuron is considered, concentrating on quantities that may be experimentally measurable but have so far received little attention. Expressions for the statistics of pre-threshold excursions, occupation density, and last crossing time of zero are compared with results from numerical generation of paths.

KEY WORDS: Noise; stochastic calculus; applied probability; dynamic bifurcation; pitchfork bifurcation; neuron dynamics; excursions; local time; threshold crossing.

1. INTRODUCTION

Differential equations have long been used to model the dynamics of physical systems. With the availability of computers, the tendency to focus only on analysis of linear equations is being replaced by a methodology that profits from a judicious mixture of numerical generation of paths, bifurcation theory and asymptotic analysis. However, when random perturbations (i.e., "noise") play an important role, this new spirit is not so widespread. One reason is that the mathematical tools appropriate for describing stochastic paths are not sufficiently well known.

In Section 2 we introduce our notation, concentrating on aspects of stochastic calculus[1-6] that may be unfamiliar to applied mathematicians. In Section 3 we consider the dynamic pitchfork bifurcation, which is of

[1] Department of Mathematics, University College London, London WC1E 6BT, England.
[2] Optique nonlinéaire théorique, Université Libre de Bruxelles CP 231, Bruxelles 1050, Belgium.

0022-4715/98/0100-0227$15.00/0

considerable interest in its own right,[8–12] and serves as an example of a system where noise of small magnitude has a disproportionate and simplifying effect.[16, 18] In Section 4 we discuss some exact results for threshold crossing problems that may be accessible to experiments but have so far received little attention. Our motivation comes from simple models for a single neuron's membrane potential[24, 25] and our intention is to introduce new ways of extracting information from numerical or experimental data.

A strong point of the stochastic approach is the close relationship between numerics and analysis. Throughout, we compare our calculations with numerical results, obtained using the algorithm described in Appendix 1.

1.1. Dynamic Bifurcations

When used to model physical systems, differential equations have parameters representing external conditions or controllable inputs. Bifurcation diagrams are used to depict the ultimate behavior of their solutions as a function of these parameters; a critical value is a point on a boundary in the space of parameters separating areas with different ultimate behavior. It is natural to speak of a bifurcation "taking place" at a critical value. Unfortunately, it is also common to speak of the qualitative behavior of the system "changing as a parameter passes through a critical value", although the paths of the nonautonomous system of differential equations obtained by letting a parameter become a function of time can differ markedly from those of the equations with fixed parameters.[8–10]

Performing the analysis of Section 3, we have in mind the following situation. Looking for a symmetry-breaking bifurcation, an experimentalist slowly changes a parameter until a qualitative change is seen. The change is seen after the parameter value at which, mathematically speaking, the bifurcation takes place; the bifurcation is said to be delayed.[8–10] Small random disturbances need to be considered explicitly to evaluate the magnitude of the delay. Previous work[13–17] on the dynamic pitchfork bifurcation has centered on the question: when do paths exceed a certain threshold distance from the former attractor? We calculate instead the last time at which this distance is zero. The cases of small and large noise are treated, and an approximate formula is presented, with the appropriate limiting behaviors, that also covers the intermediate region.

1.2. Threshold Crossing and Neuron Dynamics

Animal brains are made up of very many neurons, that communicate by firing electrical signals.[24–28] A neuron "fires" when its membrane potential

exceeds a threshold. This membrane potential, the voltage difference between the interior of the cell and its surroundings, can be measured as a function of time. It is driven away from its rest state by many thousands of excitatory and inhibitory stimuli from other neurons and is sensibly modeled by a stochastic process. We have in mind a situation where the SDE governing the neuron is not known in advance.[25] We examine the dependence of experimentally measurable quantities on the form of the SDE describing the paths until they reach a threshold, concentrating on concepts that are a natural part of stochastic calculus but not of traditional methods. The hope is that measurement of these quantities will enable the underlying dynamics to be deduced and lead to a greater understanding of single neurons and neural networks.

In Section 4, we consider the threshold crossing problem for a fairly general (non-linear) scalar SDE, but with constant threshold and noise intensity. Those sufficiently well-acquainted with the probability literature will not find new theoretical results; our purpose is to present exact results that are amenable to experimental and numerical verification, despite depending on subtle properties of the paths on small scales, and to illustrate by construction that exact results yield tractable expressions even when the underlying SDE is nonlinear. In Section 4.1 we split paths up into a series of excursions. This provides, for example, a sensitive test for asymmetries in the drift. In Section 4.2 we consider the amount of time paths spend in intervals before reaching the threshold. The function obtained in the limit where the intervals shrink to points is the local time; for a stochastic path, this is a continuous function. Section 4.3 deals with the conditioning that comes from considering only one part of a path and includes the calculation of the density of the last time at zero.

2. STOCHASTIC CALCULUS

A stochastic differential equation (SDE) is written in the following form:

$$d\mathbf{X}_t = f(\mathbf{X}_t, t)\, dt + \varepsilon(\mathbf{X}_t, t)\, d\mathbf{W}_t \tag{1}$$

Here $\mathbf{X}$ is a real-valued stochastic process; its value at time t is a real-valued random variable denoted by $\mathbf{X}_t$. If $\varepsilon(x, t)$ is always zero then (1) is just an ordinary differential equation; if $\varepsilon(x, t)$ is a real-valued function independent of x then (1) is a differential equation with additive white noise. The Wiener process $\mathbf{W}$, also called standard Brownian motion, satisfies (1) with $f(x, t) = 0$ and $\varepsilon(x, t) = 1$. Its paths are continuous with probability 1. For any $t, \Delta t \geqslant 0$, the random variable $\mathbf{W}_{t+\Delta t} - \mathbf{W}_t$ is

Gaussian with mean 0 and variance Δt, and successive increments are independent.

Random variables are in bold type in this work. For any real-valued random variable $\mathbf{a}$, the probability that $\mathbf{a} < x$ is an ordinary function of x denoted by $\mathscr{P}[\mathbf{a} < x]$. The density of $\mathbf{a}$ (if it exists) is the derivative of this function with respect to x:

$$R_{\mathbf{a}}(x) = \frac{\mathrm{d}}{\mathrm{d}x} \mathscr{P}[\mathbf{a} < x] \tag{2}$$

This is sometimes put as: $R_{\mathbf{a}}(x)\,\mathrm{d}x$ is the probability that $\mathbf{a}$ lies in $(x, x+\mathrm{d}x)$. We maintain the notation (2), with the random variable $\mathbf{a}$ as a subscript, except for the density of $\mathbf{X}_t$, when we write simply $R(x)$.

Solving an SDE on a computer consists of generating a set of values: $\{X(t_i);\ i = 1,..., n\}$, where $0 < t_1 < t_2 < \cdots < t_n = t$, that approximate the values taken by one path of $\mathbf{X}$ at the times t_i. In the lowest order algorithm $X(t_{i+1})$ is generated from $X(t_i)$ by adding a deterministic increment and a random one:

$$X(t_{i+1}) = X(t_i) = f(X(t_i), t_i)\,\Delta t + \varepsilon(X(t_i), t_i)\sqrt{\Delta t_i}\, n_i \tag{3}$$

where $\Delta t_i = t_{i+1} - t_i$ and each n_i is independently generated from a Gaussian density with mean zero and variance 1. Properties of the ensemble of paths, such as $\langle \mathbf{X}_t \rangle$, the mean value of $\mathbf{X}_t$, are estimated by repeating this procedure as many times as necessary.

In the SDE (1), the coefficient $f(x, t)$ is the mean displacement or "drift": if $\mathbf{X}_t = x$ then

$$f(x, t) = \lim_{\Delta t \to 0} \frac{1}{\Delta t} \langle \mathbf{X}_{t+\Delta t} - x \rangle \tag{4}$$

The second term on the right-hand-side of (1) and (3) does not enter (4) because it has mean zero. However, if we consider the mean squared displacement then

$$\varepsilon^2(x, t) = \lim_{\Delta t \to 0} \frac{1}{\Delta t} \langle (\mathbf{X}_{t+\Delta t} - x)^2 \rangle \tag{5}$$

Further insight is gained by making the following construction. Define sets of times $\{t_i;\ i = 0, 1,..., l\}$ such that $0 = t_0 < t_1 < \cdots < t_l = t$ and $t_{i+1} - t_i = t/l$. Choose any path of $\mathbf{X}$ and let

$$[\mathbf{X}]_t = \lim_{l \to \infty} \sum_{i=0}^{l-1} (\mathbf{X}_{t_{i+1}} - \mathbf{X}_{t_i})^2 \tag{6}$$

Then $[\mathbf{X}]$, called the quadratic variation of $\mathbf{X}$, satisfies

$$\mathrm{d}[\mathbf{X}]_t = \varepsilon^2(\mathbf{X}_t, t)\,\mathrm{d}t \tag{7}$$

(This is true of any path of $\mathbf{X}$ with probability 1.) Note that if ε is independent of $\mathbf{X}_t$ then (7) is an ordinary differential equation. The informal way to understand quadratic variation is to write

$$(\mathrm{d}\mathbf{W}_t)^2 = \mathrm{d}t \tag{8}$$

Stochastic calculus[1–6] is the calculus of (continuous but non-differentiable) paths for which the limit (6) is non-zero. If $\mathbf{X}$ and $\mathbf{Y}$ are stochastic processes obeying SDEs of the form (1), then the Itô integral,

$$\mathbf{I}_t = \int_0^t \mathbf{Y}_s \mathrm{d}\mathbf{X}_s \tag{9}$$

is itself a stochastic process given by the following limit:

$$\mathbf{I}_t = \lim_{\Delta t \to 0} \sum_{i=0}^{l-1} \mathbf{Y}_{t_i}(\mathbf{X}_{t_{i+1}} - \mathbf{X}_{t_i}) \tag{10}$$

Its quadratic variation is

$$[\mathbf{I}]_t = \int_0^t \mathbf{Y}_s^2\,\mathrm{d}[\mathbf{X}]_s \tag{11}$$

As suggested by (8), second order infinitesimals are not always negligible in stochastic calculus. This is reflected in the Itô formula, which is the chain rule of stochastic calculus. The SDE for $f(\mathbf{X})$, where f is a C^2 function, is related to that for $\mathbf{X}$ by (1–6)

$$\mathrm{d}f(\mathbf{X}_t) = f'(\mathbf{X}_t)\,\mathrm{d}\mathbf{X}_t + \tfrac{1}{2} f''(\mathbf{X}_t)\,\mathrm{d}[\mathbf{X}]_t \tag{12}$$

An alternative definition of the stochastic integral is sometimes convenient, in which $\mathbf{Y}_{t_i}$ in (10) is replaced by $\mathbf{Y}_{t_s}$, where $t_s = \frac{1}{2}(t_i + t_{i+1})$. If this alternative definition, called the Stratonovich integral, is chosen then changes of variable can be performed without the extra term that appears in (12). (An extra term appears instead in the numerical algorithm; in the Stratonovich convention, (3) no longer corresponds to the SDE (1).)

3. THE DYNAMIC PITCHFORK BIFURCATION

One of the most common transitions observed in nature is from a symmetric state to one of a set of states of lower symmetry.[12] Here we concentrate on the example of a pitchfork bifurcation, described by the normal form[21]

$$\dot{x} = gx - x^3 \tag{13}$$

If the parameter g is less than 0 the solution $x=0$ is stable; if $g>0$ it is unstable and the two states $x=\sqrt{g}$ and $x=-\sqrt{g}$ are stable. That is, for $g>0$, any small perturbation away from $x=0$ will result in the system breaking the reflection symmetry by selecting one of these states. In this work we examine what happens if g is slowly increased through 0 with white noise as the perturbation.

In a real experiment or in a numerical search of the parameter space of a set of differential equations, g will typically be a complicated function of controllable parameters. Imagine that the experiment begins with $g<0$ and that the inputs are changed in such a way that it slowly increases. In the normal form (13), x has already been scaled so that the coefficient of the cubic term is unity; we also rescale time so that the starting value of g is -1. We thus solve the SDE

$$\mathrm{d}\mathbf{X}_t = (\mu t\mathbf{X}_t - \mathbf{X}_t^3)\,\mathrm{d}t + \varepsilon\,\mathrm{d}\mathbf{W}_t, \quad \varepsilon,\mu>0, \quad t>t_0=-\frac{1}{\mu} \tag{14}$$

and derive the statistics of the last time, $\mathbf{s}$, at which $\mathbf{X}_t=0$. For convenience, we take initial condition $\mathbf{X}_{t_0}=0$. However, we shall see that the presence of noise removes the dependence on initial conditions for $\mu\,|\log\varepsilon|<1$.

Two paths of (14) are shown in Fig. 1, where $g=\mu t$. The first path lingers near $\mathbf{X}_t=0$ until $g>\sqrt{\mu}$, jumps away rather suddenly and does not return to 0. Although the path looks smooth on the scale of the figure, the moment of this jump is in fact controlled by the magnitude of the noise. The characteristic value of g for the jump,[13–16]

$$\hat{g} = \sqrt{2\mu\,|\log\varepsilon|} \tag{15}$$

is also found in the Hopf and transcritical bifurcations, and in the analogous stochastic partial differential equations with a time-dependent critical parameter.[20] These bifurcations share the property that a fixed point ceases to be an attractor, but continues to exist, after the bifurcation.[22] On the other hand, the dynamic saddle-node bifurcation, where a

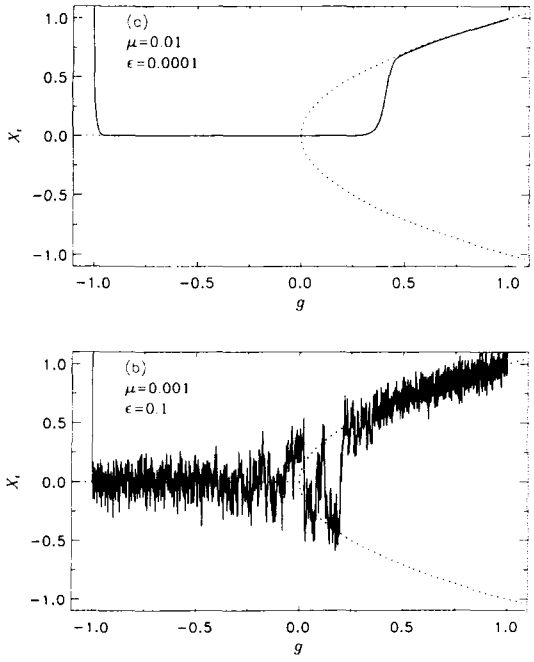

Fig. 1. *Dynamic pitchfork bifurcation.* Two paths of the SDE (14) are shown. In (a) noise is only important when $\mathbf{X}_t$ is near zero. The time of the jump away from zero is calculated from the solution of the linearized equation. Once one branch of the pitchfork is chosen, a further crossing of 0 is improbable. In (b) we treat the problem as one of jumping between minima of a potential that is slowly deepening.

fixed point ceases to exist at the critical point, has a characteristic delay that scales as $\mu^{2/3}$.[23]

The result (15) is obtained by estimating the value of g at which $\mathbf{X}_t$ is large enough that the linearized version of (14) is no longer valid. In Section 3.1, we calculate the distribution of $\mathbf{s}$ using the same method and show that it produces a good approximation for $\varepsilon \ll \sqrt{\mu}$. We also give an expression for the value of g at which the distribution of $\mathbf{X}_t$ becomes bimodal. In Section 3.2 we consider the situation, illustrated in Fig. 1(b), where paths move back and forth between branches of the pitchfork numerous times before settling down to one branch. Here we derive the density of $\mathbf{s}$ as an integral over the standard approximation for the rate of crossing between the two branches. This yields a good approximation for the density of $\mathbf{s}$ when $\varepsilon \gg \sqrt{\mu}$. We close Section 3 with a formula that interpolates between the two limits.

3.1. Linearized Equation: Small-Noise Case

The solution of the linearized version of (14) (without the cubic term) is

$$\mathbf{X}_t = e^{(1/2)\mu(t^2 - t_0^2)} \left(\mathbf{X}_{t_0} + \varepsilon \int_{t_0}^{t} e^{-(1/2)\mu(s^2 - t_0^2)} \, d\mathbf{W}_s \right) \tag{16}$$

That is, $\mathbf{X}_t$ is a Gaussian random variable with mean

$$\langle \mathbf{X}_t \rangle = e^{(1/2)\mu(t^2 - t_0^2)} \mathbf{X}_{t_0} \tag{17}$$

and variance

$$\langle \mathbf{X}_t^2 \rangle - \langle \mathbf{X}_t \rangle^2 = v(t_0, t) = \varepsilon^2 e^{\mu t^2} \int_{t_0}^{t} e^{-\mu s^2} \, ds \tag{18}$$

Suppose that $\mathbf{X}_t = x$ at some time t. Let $\mathbf{t}_h$ be the first time after t at which $\mathbf{X}$ is 0, with $\mathbf{t}_h = \infty$ if there is no such time. Note that, according to (16), $\mathbf{X}_t \to \pm\infty$ as $t \to \infty$. Because of the reflection symmetry, if the path is at zero at some time then it has an equal probability of being positive or negative at a later time. Thus the probability of never crossing zero after time t is given by

$$\mathscr{P}[\mathbf{X}_\infty > 0 \,|\, \mathbf{X}_t = x] = \tfrac{1}{2}\mathscr{P}[\mathbf{t}_h < \infty \,|\, \mathbf{X}_t = x] + \mathscr{P}[\mathbf{t}_h = \infty \,|\, \mathbf{X}_t = x] \tag{19}$$

Since $\mathscr{P}[\mathbf{t}_h = \infty \,|\, \mathbf{X}_t = x] + \mathscr{P}[\mathbf{t}_h < \infty \,|\, \mathbf{X}_t = x] = 1$, we find

$$\mathscr{P}[\mathbf{t}_h = \infty \,|\, \mathbf{X}_t = x] = 2\mathscr{P}[\mathbf{X}_\infty > 0 \,|\, \mathbf{X}_t = x] - 1 \tag{20}$$

We now evaluate the right-hand-side of (20) using (17) and (18). If $\mathbf{X}_t = x$ then, for any $T > t$, $\mathbf{X}_T$ is a Gaussian random variable with mean $m(T) = e^{(1/2)\mu(T^2 - t^2)}x$ and variance $v(t, T)$. Thus

$$2\mathscr{P}[\mathbf{X}_T > 0 \,|\, \mathbf{X}_t = x] - 1 = 2\int_0^{m(T)} (2\pi v(t, T))^{-1/2} \exp\left(-\frac{y^2}{2v(t, T)} \right) dy \tag{21}$$

Now making a change of variable in the exponent of (21) and taking the limit $T \to \infty$ gives

$$\mathscr{P}[\mathbf{t}_h = \infty \,|\, \mathbf{X}_t = x] = \operatorname{erf}\left(\frac{x}{\varepsilon} e^{-(1/2)\mu t^2} \left(2\int_t^\infty e^{-\mu s^2} \, ds \right)^{-1/2} \right) \tag{22}$$

where $\operatorname{erf}(u) = (2/\sqrt{\pi}) \int_0^u e^{-y^2} \, dy$.

The last time at zero is the random variable **s**. To calculate its density, we replace the initial condition x by a Gaussian random variable with mean 0 and variance given by (18). Then $H_1(t) = \mathscr{P}[t > \mathbf{s}]$ is obtained by integrating (22) over their Gaussian density:

$$\begin{aligned} H_1(t) &= 2\int_0^\infty \mathscr{P}[\mathbf{t}_h = \infty \mid \mathbf{X}_t = x](2\pi v(t))^{-1/2} \exp\left(-\frac{x^2}{2v(t)}\right) dx \\ &= \frac{1}{\sqrt{\pi}} \int_0^\infty e^{-u^2} \operatorname{erf}\left(u\left(\frac{\int_t^\infty \exp(-\mu s^2)\, ds}{\int_{t_0}^t \exp(-\mu s^2)\, ds}\right)^{1/2}\right) du \\ &= \frac{2}{\pi} \operatorname{atan}\left(\left(\frac{\int_t^\infty \exp(-\mu s^2)\, ds}{\int_{t_0}^t \exp(-\mu s^2)\, ds}\right)^{1/2}\right) \end{aligned} \tag{23}$$

The density of the last time, **s**, at which $\mathbf{X}_t$ passes through 0 is

$$R_s(t) = \frac{d}{dt} H_1(t) = \frac{1}{\pi} \frac{\exp(-\mu t^2)}{\left(\int_{t_0}^t \exp(-\mu s^2)\, ds \int_t^\infty \exp(-\mu s^2)\, ds\right)^{1/2}} \tag{24}$$

For $\mu \to 0$, this density is symmetric about $t = 0$ with width proportional to $1/\sqrt{\mu}$. The above calculations do not include the effect of the cubic term in (14). Because this term always pushes paths towards $\mathbf{X}_t = 0$, the function $H_1(t)$ from (23) is an upper bound on the probability of no crossing of zero after time t.

Self-consistency of the approximation (23) demands that $\mathbf{X}_t^3 \ll g\mathbf{X}_t$ for $t < (1/\sqrt{\mu})$. From (18), $\mathbf{X}_t \sim \varepsilon$ for $t < (1/\sqrt{\mu})$. Thus we require $\varepsilon \ll \sqrt{\mu}$. The calculations of this Section are quantitatively accurate when, in addition, the probability of a crossing of zero for $t \gg (1/\sqrt{\mu})$ is negligible, corresponding to the situation shown in Fig. 1(a). This assumption will be examined in the next subsection; it is also true for $\varepsilon \ll \sqrt{\mu}$.

We have used a zero initial condition in (14) because it is convenient to have $\langle \mathbf{X}_t \rangle = 0$. This initial condition corresponds to the case where the system is already close to its equilibrium before the sweep is started. With a non-zero initial condition, our calculations remain valid if $\langle \mathbf{X}_t^2 \rangle \gg \langle \mathbf{X}_t \rangle^2$ for $t > 0$. Comparison of the magnitudes of (17) (proportional to $\mathbf{X}_{t_0}$) and (18) (proportional to ε) shows that a non-zero initial condition is unimportant unless $\mathbf{X}_{t_0} > \varepsilon \exp(1/2\mu)$. This insensitivity to initial condition is characteristic of the simplification produced by noise in problems where paths sweep repeatedly past an invariant manifold.[16, 18]

The results of this Section are changed little if the noise is "colored" (i.e., if $\mathbf{W}_t$ in (14) is replaced by a stochastic process whose increments are correlated).[19] If a deterministic perturbation is used instead of noise, the

effect is proportional to the mean of the perturbation. Multiplicative noise is less important than additive noise.[19, 20]

3.1.1. Transition to Bimodal Density. To estimate when nonlinear terms become important in a dynamic bifurcation, one can calculate from the linearized version the time when $\mathbf{X}_t$ exceeds some threshold.[13–16] Here, we calculate instead, from the nonlinear equation with $\varepsilon \ll \sqrt{\mu} \ll 1$, the time when the distribution of $\mathbf{X}_t$ changes from unimodal (one maximum at 0) to bimodal. We do this by considering the evolution of an ensemble of paths from a Gaussian distribution of initial conditions into the latter part of the path where $|\mathbf{X}_t| \to \sqrt{g}$ from below. Effectively, noise provides a random initial condition for the subsequent, deterministic, evolution.

The solution of the deterministic equation,

$$\dot{x} = \mu t x - x^3 \tag{25}$$

with initial condition $x = x_1$ at $t = t_1$ is:

$$x = \frac{x_1}{|x_1|} \mathrm{e}^{(1/2)\mu(t^2 - t_1^2)} \left(x_1^{-2} + 2 \int_{t_1}^{t} \mathrm{e}^{\mu(s^2 - t_1^2)} \, \mathrm{d}s \right)^{1/2} \tag{26}$$

Now, instead of a constant as initial condition, we take the following Gaussian random variable:

$$\mathbf{X}_{t_1} = w(t_1)\, \mathbf{n}, \qquad \text{where} \quad w(t) = \varepsilon \left(\frac{\pi}{\mu} \right)^{1/4} \mathrm{e}^{(1/2)\mu t^2} \tag{27}$$

is the large-t limit of $v(t)$ (18), and $\mathbf{n}$ is a Gaussian random variable with mean 0 and variance 1. We use $2\int_{t_1}^{t} \exp(\mu s^2)\, \mathrm{d}s \simeq \exp(\mu t^2)(\mu t)^{-1}$ and obtain

$$\mathbf{X}_t^{\,2} = \left(\frac{1}{w^2(t)\, \mathbf{n}^2} + \frac{1}{\mu t} \right)^{-1} \tag{28}$$

The density of $\mathbf{X}_t$ is then given, with t as a parameter, by

$$R(x) = \sqrt{\frac{2}{\pi}}\, w(t) \exp\left(\frac{-x^2}{2w(t)^2 (1 - x^2/\mu t)} \right) \left(1 - \frac{x^2}{\mu t} \right)^{-3/2} \tag{29}$$

it has a maximum at a non-zero value of x if $w^2(t) > (1/3)\mu t$. The time when the density changes to bimodal therefore satisfies

$$(\mu t)^2 - \mu \log \frac{\mu t}{3} = 2\mu\, |\log \varepsilon| + \frac{\mu}{2} \log \frac{\pi}{\mu} \tag{30}$$

For small μ, we recover the result $(\mu t)^2 = 2\mu\,|\log \varepsilon|$ that comes from the analysis of the linearized system with a fixed threshold.[13-16]

3.2. Effect of the Cubic Term: Large-Noise Case

The probability that there is no crossing of zero after time t is a positive increasing function of time, $H(t)$. We can therefore make the decomposition

$$\frac{\mathrm{d}}{\mathrm{d}t} H(t) = r(t)\, H(t) \tag{31}$$

So

$$H(t) = \exp\left(-\int_t^\infty r(s)\, \mathrm{d}s \right) \tag{32}$$

The function $r(t)$ is everywhere positive and can be interpreted as the probability per unit time of a crossing of zero. In Section 3.1 we obtained an upper bound on $H(t)$ from the linearized equation. A lower bound on $H(t)$ can be obtained as follows. Calculate the probability per unit time of a crossing of zero from (14) with μt taken as a fixed parameter. Denote this function by $r_2(t)$. Because the slow increase of g makes crossings of zero rarer as t increases, $r_2(t)$ is an upper bound on the rate of zero crossings. The function $H_2(t)$, calculated from (32), is therefore a lower bound on the exact result $H(t)$. For direct comparison with numerics, $H_2(t)$ is obtained by integrating $r_2(t)$ over the density of $\mathbf{X}_t$; this result is an unwieldy expression. Here we restrict ourselves to the case $g > \varepsilon$ and examine the validity of the compact expression that results.

The expression (31) is most useful and intuitive for $g > \varepsilon$, when paths spend most of their time near $\pm\sqrt{g}$. Then $r_2(t)$ is well approximated by the inverse of the mean passage time from $\mathbf{X}_t = \pm\sqrt{g}$ to $\mathbf{X}_t = 0$:[1, 22]

$$r_2(t) = \frac{\sqrt{2}}{\pi}\, g \exp\left(-\frac{g^2}{2\varepsilon^2} \right) \tag{33}$$

Using (33) in (31) with $g = \mu t$ gives

$$H_2(t) = \frac{\sqrt{2}}{\pi} \exp\left(-\frac{\sqrt{2}}{\pi} \frac{\varepsilon^2}{\mu} \exp\left(\frac{g^2}{2\varepsilon^2} \right) \right) \tag{34}$$

The expression for the density of $\mathbf{s}$ corresponding to (34) is

$$R_{\mathbf{s}}(t)=\frac{\mathrm{d}}{\mathrm{d}t}H_2(t)=\frac{\sqrt{2}}{\pi}g\exp\left(-\frac{g^2}{2\varepsilon^2}\right)\exp\left(-\frac{\sqrt{2}}{\pi}\frac{\varepsilon^2}{\mu}\exp\left(-\frac{g^2}{2\varepsilon^2}\right)\right) \tag{35}$$

As $\mu\to 0$, the mean value of $\mathbf{s}$ is[16]

$$\langle\mathbf{s}\rangle=\frac{1}{\mu}\left(g^*+\gamma\frac{\varepsilon^2}{g^*}\right)\qquad\text{where}\quad g^*=\varepsilon\left(2\log\left(\frac{\sqrt{2}\,\varepsilon^2}{\pi\mu}\right)\right)^{1/2} \tag{36}$$

and Euler's constant $\gamma=0.57721....$ In the same limit, the standard deviation is

$$(\langle\mathbf{s}^2\rangle-\langle\mathbf{s}\rangle^2)^{1/2}=\frac{\varepsilon\pi}{\mu\sqrt{12}}\left(\log\frac{\sqrt{2}\,\varepsilon^2}{\pi\mu}\right)^{-1/2} \tag{37}$$

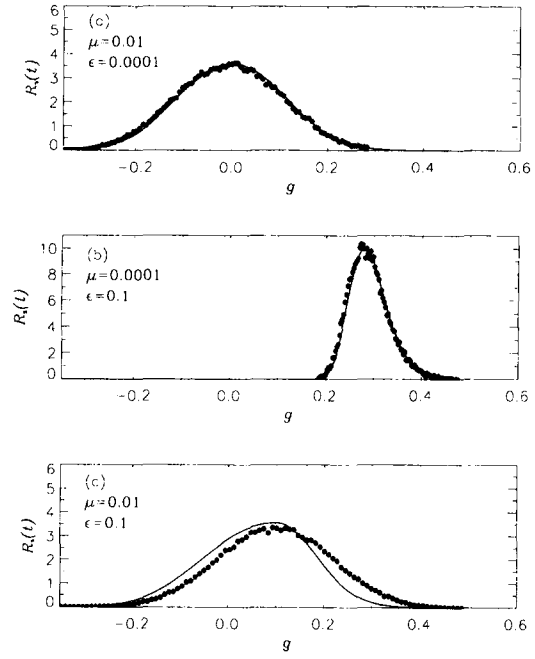

Fig. 2. *Last crossing of zero: numerical results vs formula.* The dots are the histogram compiled from numerical generation of 10000 paths of (14) and the solid lines are the uniform approximation described in Section 3.3. Figure (a) exhibits the small-noise case ($\varepsilon<\sqrt{\mu}$) and (b) the large-noise case. Note $g=\mu s$.

The approximations (33)–(37) are valid if $g^* \gg \varepsilon$, which is true if $\varepsilon > \sqrt{\mu}$. Note also that $H_2(t) \simeq 1$ for $g \geqslant \sqrt{\mu}$ if $\varepsilon < \sqrt{\mu}$, as required for validity of the calculations of Section 3.1.

The decomposition (31) also provides a natural way to unify the above approximation with that of Section 3.1. Let $r(t) = r_1(t) + r_2(t)$ where $r_1(t) = H_1(t)^{-1} (\mathrm{d}/\mathrm{d}t) H_1(t)$, with $H_1(t)$ given by (23). Then $H(t)$ can be obtained from (32). This yields the following approximation to $R_s(t)$ that has (35) and (24) in the large-noise and small-noise regimes:

$$\begin{aligned} R_s(t) &= (r_1 + r_2) H_1 H_2 \\ &= H_2(t) \frac{\mathrm{d}}{\mathrm{d}t} H_1(t) + H_1(t) \frac{\mathrm{d}}{\mathrm{d}t} H_2(t) \end{aligned} \tag{38}$$

In Fig. 2, we used

$$r_2(t) = \begin{cases} \dfrac{\sqrt{2}}{\pi} g \exp\left(-\dfrac{g^2}{2\varepsilon^2}\right) & g \geqslant \varepsilon \\ \dfrac{\sqrt{2}}{\pi} \varepsilon \exp\left(-\dfrac{1}{2}\right) & g < \varepsilon \end{cases} \tag{39}$$

4. EXACT RESULTS ON THRESHOLD CROSSINGS

In this Section we consider stochastic processes obeying SDEs of the following type:

$$\mathrm{d}\mathbf{X}_t = f(\mathbf{X}_t)\,\mathrm{d}t + \mathrm{d}\mathbf{W}_t \tag{40}$$

with initial condition $\mathbf{X}_0 = 0$. Paths are followed until the first time, $\mathbf{t}_b$, that they reach a threshold $b > 0$. If $f(x)$ is not known in advance, what can be learned from the paths of $\mathbf{X}_t$ for $t < \mathbf{t}_b$? The process $\mathbf{X}_t$ models, for example, the membrane potential of a neuron[24, 30] or the path of a diffusing particle.[31] To produce (40) from the more general SDE (1), we assume that ε is constant. We can then scale time so that the coefficient of the second term in (1) is 1. We also primarily consider the case where the drift, $f(x)$, is towards $x = 0$.

We do not calculate two of the quantities traditionally considered by theorists: the density of $\mathbf{X}_t$ and that of $\mathbf{t}_b$.[27, 28] We calculate instead quantities that are measurable by an experimentalist who can record individual

paths, but have so far received little attention outside of probability theory. All quantities calculated are derived from the following function:

$$S(x) = \begin{cases} \int_0^x \exp(2U(y))\,\mathrm{d}y & x \geqslant 0 \\ \int_x^0 \exp(2U(y))\,\mathrm{d}y & x < 0 \end{cases} \tag{41}$$

where

$$U(x) = -\int_0^x f(y)\,\mathrm{d}y \tag{42}$$

The function $S(x)$ is generated on a computer by solving the ordinary differential equation

$$\begin{aligned} S'(x) &= \exp(2U(x)) & x > 0 \\ S(0) &= 0 \\ S'(x) &= -\exp(2U(x)) & x < 0 \end{aligned} \tag{43}$$

Further, $S(x)$ has the following simple interpretation. Given $\mathbf{X}_t = x$, $0 \leqslant x \leqslant b$, at some time, the probability that $\mathbf{X}$ reaches b before 0 is $(S(x)/S(b))$. An advantage for performing calculations is that $S(x)$ is time-independent. This is a consequence of the "memoryless" property of paths of the SDE: the future of $\mathbf{X}_t$ depends only on the value of $\mathbf{X}_t$, not on the path before this time. In the traditional approach, based on the Fokker–Planck equation, measurable quantities are derived from the density of $\mathbf{X}_t$, which is time-dependent because of the flux of probability through the threshold.

A path of a stochastic process obeying the SDE (40) can be thought of as being made up of a series of excursions from zero. Each time $\mathbf{X}_t$ returns to 0 the process is considered as starting afresh, and each excursion treated as an independent event.[2–5] In Section 4.1 we derive the statistics of the excursions in terms of the maximum distance from the origin during the excursion.

In Section 4.2 we use the concept of local time, which measures the occupation density of a path.[3–5, 32] Given a path of a stochastic process satisfying (40), the local time at a is a stochastic process whose value at time t is given by

$$\mathbf{L}_t(a) = \lim_{\Delta a \to 0} \frac{1}{2\Delta a} \int_0^t \mathscr{I}\{\mathbf{X}_s \in (a - \Delta a, a + \Delta a)\}\,\mathrm{d}s \tag{44}$$

where $\mathscr{I}\{\Theta\} = 1$ if Θ is true and is zero otherwise. Note that for fixed a, $\mathbf{L}_t(a)$ increases at times when $\mathbf{X}_t = a$ and is constant otherwise.

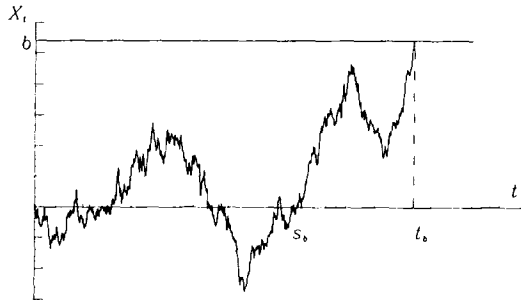

Fig. 3. *Threshold crossing.* The first time a path attains a level b is a random variable, denoted by $\mathbf{t}_b$. Also indicated is $\mathbf{s}_b$, the last time before $\mathbf{t}_b$ at which the path is at 0. The path shown is a path of the Wiener process.

Local time is the limit of functions that can be constructed from a series of values of $\mathbf{X}_t$ that could be available to an experimentalist. Suppose the amount of time spent in boxes $(a-\Delta a, a+\Delta a)$ before $\mathbf{t}_b$ is recorded. The function obtained in the limit $\Delta a \to 0$ is $\mathbf{L}_{\mathbf{t}_b}(a)$. In Section 4.2 we consider two ways of comparing numerical or theoretical data with $\mathbf{L}_{\mathbf{t}_b}(a)$: as an average over many paths and for one path at a time.

In Section 4.3 we consider the portion of the path of $\mathbf{X}$ after $\mathbf{s}_b$, the last time that the path passes through zero before $\mathbf{t}_b$. This is convenient, both numerically and experimentally, when $\mathbf{t}_b$ is large: rather than generating or recording the whole path, one can concentrate on only the last portion. Further, it is one case where calculations based on a constant threshold will be a good approximation to the case where the threshold approaches a constant value for large t.

4.1. Excursions

An excursion is a portion of a path between successive crossings of 0. A path can be thought of as consisting of a series of excursions occurring one after the other, with properties chosen according to a certain probability. We construct this probability as follows. For $x>0$, let $N(x)$ be the number of excursions before $\mathbf{s}_b$ (see Fig. 3) during which the maximum of $\mathbf{X}$ is greater than x; for $x<0$, let $N(x)$ be the corresponding number of excursions with minimum less than x.

Suppose that at some time t, $\mathbf{X}_t = x > 0$. Then the probability that $\mathbf{X}$ reaches b before 0 is $S(x)/S(b)$. Thus

$$\mathscr{P}[N(x)=n] = \frac{S(x)}{S(b)}\left(1-\frac{S(x)}{S(b)}\right)^n \qquad x>0 \tag{45}$$

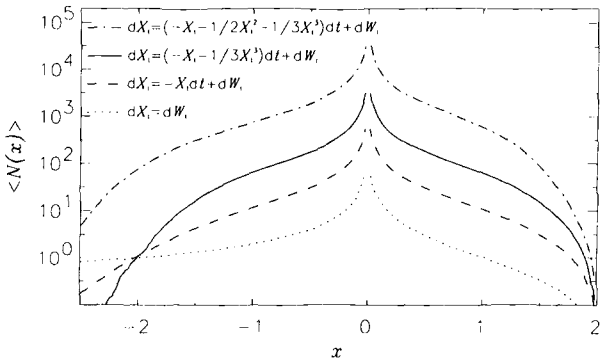

Fig. 4. *Pre-threshold excursions.* Here $\langle N(x) \rangle$ is the average number of excursions with maximum greater than $|x|$ before $\mathbf{t}_b (b = 2)$. The curves, produced by averaging over 100 numerically-produced paths with $\Delta t = 10^{-4}$, are in excellent agreement with the exact result (47).

Now consider $x < 0$ and suppose that at some time t, $\mathbf{X}_t = 0$. Then the probability that $\mathbf{X}$ reaches x before b is $S(b)/(S(x) + S(b))$. Thus

$$\mathscr{P}[N(x) = n] = \frac{S(x)}{S(x) + S(b)} \left(\frac{S(b)}{S(x) + S(b)} \right)^n \qquad x < 0 \tag{46}$$

From (45) and (46) we find the following exact result for the mean of $N(x)$:

$$\langle N(x) \rangle = \begin{cases} \dfrac{S(b)}{S(x)} & x < 0 \\ \infty & x = 0 \\ \dfrac{S(b)}{S(x)} - 1 & x > 0 \end{cases} \tag{47}$$

We find good agreement between the exact result (47) and averages over paths of generated with a finite time-step (see Fig. 4). Note that, if the drift $f(x)$ is symmetric, then $\langle N(-b) \rangle = 1$. This is a sensitive test for asymmetries in $f(x)$. We have not counted the portion of the path after $\mathbf{s}_b$ as an excursion. We return to this in Section 4.3.

4.2. Occupation Density

Another way to extract information from a path followed until it reaches a threshold is to construct the occupation density: the amount of

time spent in boxes $(a-\Delta a, a+\Delta a)$ before $\mathbf{t}_b$. The function obtained in the limit $\Delta a \to 0$ is $\mathbf{L}_{\mathbf{t}_b}(a)$, the local time for a path run until it first reaches the threshold b. For convenience, in this section we denote $\mathbf{L}_{\mathbf{t}_b}(a)$ simply by $\mathbf{L}_a$.

We first consider the local time, averaged over many paths. Given $\mathbf{X}_0 = x$, $c < x < b$, let $l(x)$ be the mean value of the local time at a before the first time that $\mathbf{X}_t$ exits the interval (c, b). Using the delta-function notation to rewrite (44),

$$\mathbf{L}_a = \int_0^{\mathbf{t}_b} \delta(\mathbf{X}_s - a)\, \mathrm{d}[\mathbf{X}]_s \tag{48}$$

we find (see Appendix 2) that $l(x)$ satisfies:

$$-\delta(a) = f(x)\, l'(x) + \tfrac{1}{2} l''(x), \quad l(c) = l(b) = 0 \tag{49}$$

With $x = 0$ and $c = -\infty$ we obtain $\langle \mathbf{L}_a \rangle$ from the solution of (49):

$$\langle \mathbf{L}_a \rangle = \begin{cases} 2\exp(-2U(a))(S(b) - S(a)) & a \geqslant 0 \\ 2\exp(-2U(a))\, S(b) & a < 0 \end{cases} \tag{50}$$

This average is displayed for several choices of $f(x)$ in Fig. 5.

The average (50) is an average over realizations and thus is useful when many paths have been recorded. Quantitative comparison can also be performed for just a few paths, exploiting the fact that an occupation density can be constructed from just one path. A remarkable fact is

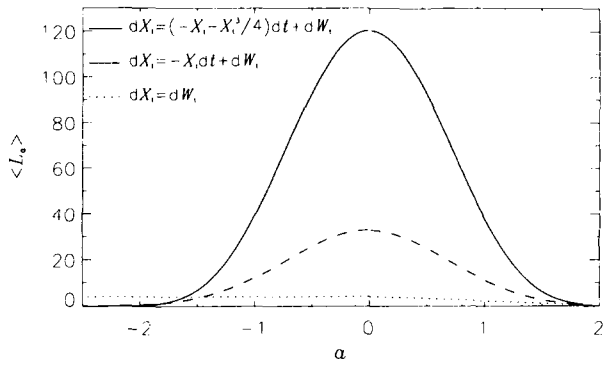

Fig. 5. *Average occupation density.* The curves are (50), the analytical result for the average (over many paths) of the amount of time spent at a before the first time that a path, started at 0, reaches $b = 2$.

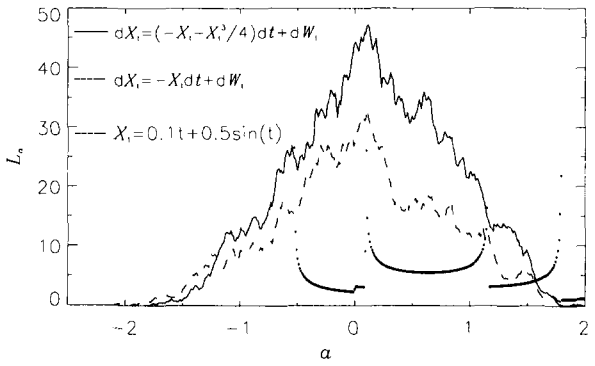

Fig. 6. *Occupation density.* Each curve was obtained by following one path until it reached $b=2$. We used $\Delta a=0.01$ and $\Delta t=10^{-5}$. Note the discontinuities in $\mathbf{L}_a$ for the deterministic path.

illustrated in Fig. 6: $\mathbf{L}_a$ is a continuous function of a when $\varepsilon \neq 0$. In fact, $\mathbf{L}_a$ can be considered as a stochastic process *indexed by the space variable a.* In Appendix 3 we show that $\mathbf{L}_a$ satisfies the non-autonomous SDE[29]

$$d\mathbf{L}_z = \begin{cases} 2\mathbf{L}_z^{1/2}\, d\mathbf{W}_z - 2(f(b-z)\,\mathbf{L}_z - 1)\, dz & z \leqslant b \\ 2\mathbf{L}_z^{1/2}\, d\mathbf{W}_z - 2f(b-z)\,\mathbf{L}_z\, dz & z > b \end{cases} \tag{51}$$

where $z=b-a$. Traces mimicking those of Fig. 6 can therefore be directly generated by solving (51) with the initial condition $\mathbf{L}_0=0$. The drift of the SDE (51) ensures that $\mathbf{L}_z$ remains positive for $z<b$ $(a>0)$; a path is followed until $\mathbf{L}_z=0$ for some $z>b$ $(a<0)$.

For $a>0$, the density of the random variable $\mathbf{L}_a$ is

$$R_{\mathbf{L}_a}(y) = \langle \mathbf{L}_a \rangle^{-1/2} \exp\left(-\frac{y}{\langle \mathbf{L}_a \rangle}\right) \tag{52}$$

with $\langle \mathbf{L}_a \rangle$ given by (50). The corresponding result for $a<0$ is

$$\mathscr{P}[\mathbf{L}_a = 0] = \frac{S(a)}{S(a)+S(b)} \tag{53}$$

$$R_{\mathbf{L}_a}(y) = \frac{S(b)}{S(a)+S(b)} \frac{1}{q(a)} \exp\left(-\frac{y}{q(a)}\right) \quad y>0 \tag{54}$$

where $q(a)=2\exp(-2U(a))(S(a)+S(b))$.

4.3. Last Zero Crossing

When $\mathbf{t}_b$ is large, it may be impractical experimentally to record the whole path until $\mathbf{t}_b$. Numerically, it also becomes time-consuming to generate enough paths to evaluate averages. One way around this is to concentrate on the portion of the path between $\mathbf{s}_b$, the last time that the path passes through zero, and $\mathbf{t}_b$. Numerically, it is possible to generate this portion of the path directly.

Generating one portion of a path conditioned on desired properties is equivalent to selecting a subset of possible paths (here, paths that do not return to 0). This is equivalent to changing the drift of the SDE. Define $\mathbf{Y}$ to be the conditioned process and suppose $\mathbf{X}_t = x$ at some t. Then the probability that $t > \mathbf{s}_b$ is $h(x) = (S(x)/S(b))$. That is, the probability that a path of $\mathbf{X}$ with $\mathbf{X}_t = x$ is also a path of $\mathbf{Y}$ is $h(x)$. Let $\Delta\mathbf{X} = \mathbf{X}_{t+\Delta t} - \mathbf{X}_t$. Then the drift of the SDE for $\mathbf{Y}$ is

$$\begin{aligned}\lim_{\Delta t \to 0} \frac{1}{\Delta t} \langle \mathbf{Y}_{t+\Delta t} - x \rangle &= \lim_{\Delta t \to 0} \frac{1}{\Delta t} \frac{\langle h(x+\Delta\mathbf{X})\, \Delta\mathbf{X} \rangle}{\langle h(x+\Delta\mathbf{X}) \rangle} \\ &= \lim_{\Delta t \to 0} \frac{1}{\Delta t} \frac{\langle (h(x) + h'(x)\, \Delta\mathbf{X} + \cdots)\, \Delta\mathbf{X} \rangle}{h(x)} \\ &= \lim_{\Delta t \to 0} \frac{1}{\Delta t} \langle \mathbf{X}_{t+\Delta t} - x \rangle + \frac{S'(x)}{S(x)} \end{aligned} \tag{55}$$

Because we are choosing a subset of paths with non-zero probability, the rate of increase of quadratic variation (which is the same for each path) is not affected by the conditioning. The SDE for $\mathbf{Y}_s$ is thus

$$d\mathbf{Y}_s = \tilde{f}(\mathbf{Y}_s)\, ds + d\mathbf{W}_s \qquad \text{where} \quad \tilde{f}(y) = f(y) + \frac{S'(y)}{S(y)} \tag{56}$$

The transformed drift $\tilde{f}(x)$ is singular at $x = 0$, which has the required effect of preventing paths of $\mathbf{Y}$ from returning to 0. (Note the following relationship between f and $\tilde{f}$:

$$\tilde{f}'(x) = f'(x) - \tilde{f}^2(x) + f^2(x) \tag{57}$$

The boundary condition for (57) is $x\tilde{f}(x) \to 1$ as $x \to 0$.)

From the transformed drift, quantities such as $\tilde{U}'(y) = -\tilde{f}(y)$ can be defined and calculated as described in this section. For example, the mean

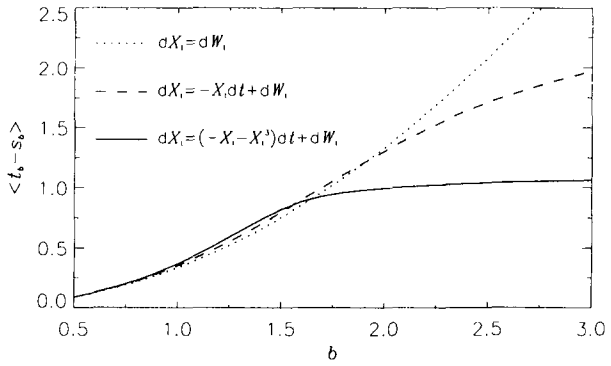

Fig. 7. *Last zero crossing.* The curves are $\mathbf{t}_b - \mathbf{s}_b$ versus the height of the boundary b for various choices of the drift $f(x)$. They are produced by integrating the expression (59).

value of $\mathbf{t}_b - \mathbf{s}_b$ is the mean first passage time from $\mathbf{Y} = 0$ to $\mathbf{Y} = b$, which is given by (Appendix 2):

$$\langle \mathbf{t}_b - \mathbf{s}_b \rangle = \lim_{x \to 0} 2 \int_x^b \exp(2\tilde{U}(y)) \int_0^y \exp(-2\tilde{U}(z))\, dz\, dy$$

$$= \lim_{x \to 0} 2 \int_x^b \frac{1}{S^2(y)} \exp(2U(y)) \int_0^y S^2(z) \exp(-2U(z))\, dz\, dy \quad (58)$$

In Fig. 7 this mean is displayed as a function of the threshold b for several examples of $f(x)$.

5. CONCLUSION

If a symmetry-breaking bifurcation is searched for by making a parameter a function of time, the delay produced means that it is not obvious how to define or measure its position using standard ideas. The presence of noise simplifies the picture by removing the dependence on initial conditions in the limit of small sweep rate, but means that the usual criteria for determining the position of the bifurcation, based on deterministic differential equations, are no longer appropriate.[22] We study the dynamic pitchfork bifurcation and choose a simple concept: the last time, $\mathbf{s}$, that a path is at zero. The density of $\mathbf{s}$ is calculated as a function of the noise level, ε, and the rate of change of the parameter, μ. If $\varepsilon \ll \sqrt{\mu}$, there is a neat separation between the noise-dominated and nonlinear parts of the path. The mean of $\mathbf{s}$ in this case is the point of loss of stability as calculated by static theory and the standard deviation of $\mathbf{s}$ is proportional

to $\mu^{-1/2}$. An expression is also calculated for the time when the density of $\mathbf{X}_t$ becomes two-humped. Here the result is consistent with those obtained by setting a threshold on $\mathbf{X}_t$: the characteristic delay of the bifurcation is $\sqrt{2\mu\,|\log\varepsilon|}$. In the second case, $\varepsilon \gg \sqrt{\mu}$, the analysis is analogous to that of a two-state system. The mean value of $\mathbf{s}$ is a slowly increasing function of μ and ε, and the standard deviation of $\mathbf{s}$ is proportional to ε. Numerical results are compared with a uniform approximation that captures these two cases as limits.

A threshold crossing problem is the ideal setting for stochastic methods. In Section 4, we consider some exact results and compare them with numerical data. Our aim is to calculate quantities that an experimentalist, confronted with a series of paths like that of Fig. 3, can use to deduce the underlying dynamics. The particular motivation comes from the modeling of neurons that fire when their membrane potential exceeds a threshold. Results are expressed in terms of the function $S(x)$ (41), which is easily generated on a computer.

APPENDICES

1. Numerical Methods

As suggested by the SDE notation (1), the simplest algorithm for solving an SDE is the following. At each step add two increments to $\mathbf{X}_t$: a drift given by $f(\mathbf{X}_t, t)\,\Delta t$, where Δt is the timestep, and another that is a random variable proportional to $\varepsilon\sqrt{\Delta t}$. The stochastic version of the Euler method for constructing an approximation X_t to $\mathbf{X}_t$ is:

$$X_{t+\Delta t} = X_t + f(X_t, t)\,\Delta t + \varepsilon(X_t, t)\sqrt{\Delta t}\,n \tag{59}$$

where n is a Gaussian random variable with mean zero and variance 1. The method that was used to generate the figures in this work is analogous to the second-order Runge–Kutta method:[33]

$$\begin{aligned} X_{t+\Delta t} = X_t + \tfrac{1}{2}(f(X_t, t) + f(X_t + f(X_t, t)\,\Delta t \\ + \varepsilon\sqrt{\Delta t}\,n, t + \Delta t))\,\Delta t + \varepsilon\sqrt{\Delta t}\,n. \end{aligned} \tag{60}$$

Note that only one Gaussian random variable is generated at each time step. For the algorithm (60) there exist positive constants κ and δ such that, if ε is constant and if the step size Δt is less than δ, then $|\langle h(X_t)\rangle - \langle h(\mathbf{X}_t)\rangle| \leqslant \kappa(\Delta t)^2$ for any polynomial function h. Higher order algorithms exist.[6]

2. Derivation of PDEs from the Itô Formula

Consider the SDE

$$\mathrm{d}\mathbf{X}_t = f(\mathbf{X}_t)\,\mathrm{d}t + \varepsilon\,\mathrm{d}\mathbf{W}_t, \quad \mathbf{X}_0 = x, \quad a < x < b \tag{61}$$

and define $T(x)$ to be the mean value of the first time that $\mathbf{X}_t = b$. Since $T(x)$ is an ordinary function of the initial condition x, we can consider the evolution of $T(\mathbf{X}_t)$ along a path. The SDE for $T(\mathbf{X}_t)$ is, using the Itô formula (12):

$$\mathrm{d}T(\mathbf{X}_t) = \frac{\partial T}{\partial x}(\mathbf{X}_t)\,\mathrm{d}X_t + \frac{1}{2}\varepsilon^2 \frac{\partial^2 T}{\partial x^2}(\mathbf{X}_t)\,\mathrm{d}[\mathbf{X}]_t \tag{62}$$

We know, from the definition of $T(x)$, that

$$\langle \mathrm{d}T(\mathbf{X}_t)\rangle = -\mathrm{d}t \tag{63}$$

From (7), the quadratic variation for the process $\mathbf{X}_t$ satisfies $\mathrm{d}[\mathbf{X}_t] = \varepsilon^2\,\mathrm{d}t$ and, from (4), $\langle \mathrm{d}\mathbf{X}_t\rangle = f(\mathbf{X}_t)\,\mathrm{d}t$. Thus taking the mean value of both sides of (62) gives[1, 2]

$$\frac{1}{2}\varepsilon^2 \frac{\partial^2 T}{\partial x^2} + f(x)\frac{\partial T}{\partial x} = -1, \quad T(a) = T(b) = 0 \tag{64}$$

In Section 4, we also consider the quantities $h(x)$, the probability that $\mathbf{X}$ reaches b before a, and $l(x)$, the mean value of $\mathbf{L}_{t_b}(a)$. The appropriate PDEs are derived as above, using $\langle \mathrm{d}h(\mathbf{X}_t)\rangle = 0$ and $\langle \mathrm{d}l(\mathbf{X}_t)\rangle = -\delta(a)\,\mathrm{d}t$ instead of (63).

3. SDE for Local Time in Space Variable

As in Section 4.2, $\mathbf{L}_a$ denotes the local time at a (44), evaluated at $t = \mathbf{t}_b$. We consider $\mathbf{L}_a$ as a stochastic process indexed by a and derive the corresponding SDE. By differentiating (50), the drift of the SDE for $\mathbf{L}_a$ is:

$$\frac{\mathrm{d}}{\mathrm{d}a}\langle \mathbf{L}_a\rangle = \begin{cases} 2(f(a)\,\mathbf{L}_a - 1) & a \geqslant 0 \\ 2f(a)\,\mathbf{L}_a & a < 0 \end{cases} \tag{65}$$

To find the quadratic variation of $\mathbf{L}_a$, we begin by using Itô's formula to derive an SDE for the function $u(\mathbf{X}_t)$ where $\mathbf{X}_t$ satisfies (40) and

$$u(x) = \begin{cases} x & x \geqslant a \\ a & x < a \end{cases} \tag{66}$$

Note that $u''(x)=\delta(x-a)$. The SDE for $u(\mathbf{X}_t)$ is

$$\mathrm{d}u(\mathbf{X}_t)=\mathscr{I}\{\mathbf{X}_t>a\}\,\mathrm{d}\mathbf{X}_t+\tfrac{1}{2}\delta(\mathbf{X}_t-a)\,\mathrm{d}t \tag{67}$$

Integrating (67) yields

$$u(\mathbf{X}_t)-u(\mathbf{X}_0)=\int_0^t \mathscr{I}\{\mathbf{X}_t>a\}\,\mathrm{d}\mathbf{X}_t+\frac{1}{2}\int_0^t \delta(\mathbf{X}_t-a)\,\mathrm{d}t \tag{68}$$

Choosing $t=\mathbf{t}_b$ and $\mathbf{X}_0=0$ gives

$$u(b)-u(0)=\int_0^{\mathbf{t}_b}\mathscr{I}\{\mathbf{X}_t>a\}\,\mathrm{d}\mathbf{X}_t+\frac{1}{2}\,\mathbf{L}_{\mathbf{t}_b}(a) \tag{69}$$

Thus

$$\mathbf{L}_a=2\mathbf{Z}_a+2(u(b)-u(0)) \qquad \text{where} \quad \mathbf{Z}_a=\int_0^{\mathbf{t}_b}\mathscr{I}\{\mathbf{X}_t>a\}\,\mathrm{d}\mathbf{X}_t \tag{70}$$

Now define a set $\{a_i;\, i=0,1,\ldots,l\}$ such that $a=a_0<a_1<\cdots<a_l=b$ and $a_{i+1}-a_i=(b-a)/l$ and denote the quadratic variation of $\mathbf{L}_a$ by $[\mathbf{L}]_a$. Then

$$\begin{aligned}[\mathbf{L}]_a&=\lim_{l\to\infty}\sum_{i=0}^{l-1}(\mathbf{L}_{a_{i+1}}-\mathbf{L}_{a_i})^2\\&=\lim_{l\to\infty}\sum_{i=0}^{l-1}4(\mathbf{Z}_{a_{i+1}}-\mathbf{Z}_{a_i})^2\end{aligned} \tag{71}$$

To evaluate (71), we define the processes $\mathbf{Q}_t^{(i)}=(\int_0^t \mathscr{I}\{a_i<\mathbf{X}_t<a_{i+1}\}\,\mathrm{d}\mathbf{X}_t)^2$. Then $\mathbf{Q}_{\mathbf{t}_b}^{(i)}=(\mathbf{Z}_{a_{i+1}}-\mathbf{Z}_{a_i})^2$. The SDE for $\mathbf{Q}_t^{(i)}$ is, using Itô's formula,[5, 29]

$$\begin{aligned}\mathrm{d}\mathbf{Q}_t^{(i)}=2\left(\int_0^t \mathscr{I}\{a_i<\mathbf{X}_t<a_{i+1}\}\,\mathrm{d}\mathbf{X}_t\right)\mathscr{I}\{a_i<\mathbf{X}_t<a_{i+1}\}\,\mathrm{d}\mathbf{X}_t\\+\mathscr{I}\{a_i<\mathbf{X}_t<a_{i+1}\}\,\mathrm{d}t\end{aligned} \tag{72}$$

Thus

$$\begin{aligned}\mathbf{Q}_{\mathbf{t}_b}^{(i)}=2\int_0^{\mathbf{t}_b}(\mathbf{Z}_{a_{i+1}}-\mathbf{Z}_{a_i})\,\mathscr{I}\{a_i<\mathbf{X}_t<a_{i+1}\}\,\mathrm{d}\mathbf{X}_t\\+\int_0^{\mathbf{t}_b}\mathscr{I}\{a_i<\mathbf{X}_t<a_{i+1}\}\,\mathrm{d}t\end{aligned} \tag{73}$$

In the large-l limit, only the contributions to $[\mathbf{L}]_a$ from the second integral in (73) remain[5, 29] and

$$[\mathbf{L}]_a = 4\int_0^{t_b} \mathscr{I}\{\mathbf{x}_t > a\}\,\mathrm{d}t \tag{74}$$

$$= 4\int_a^b \mathbf{L}_x\,\mathrm{d}x$$

Thus, defining $z = b - a$, $\mathbf{L}_z$ satisfies the SDE[29]

$$\mathrm{d}\mathbf{L}_z = \begin{cases} 2\mathbf{L}_z^{1/2}\,\mathrm{d}W_z - 2(f(b-z)\,\mathbf{L}_z - 1)\,\mathrm{d}z & z \leqslant b \\ 2\mathbf{L}_z^{1/2}\,\mathrm{d}W_z - 2f(b-z)\,\mathbf{L}_z\,\mathrm{d}z & z > b \end{cases} \tag{75}$$

with initial condition $\mathbf{L}_0 = 0$ and an absorbing boundary at 0.

ACKNOWLEDGMENTS

We are grateful for the encouragement of Mike Proctor, Nigel Weiss and Jerôme Losson.

REFERENCES

1. W. Gardiner, *Handbook of stochastic methods* (Springer, Berlin, 1990).
2. S. Karlin and H. M. Taylor, *A second course in stochastic processes* (Academic, Orlando, 1981).
3. L. C. G. Rogers and D. Williams, *Diffusions, Markov Processes and Martingales. Vol. 2: Itô calculus* (Wiley, Chichester, 1987).
4. I. Karatzas and S. E. Shreve, *Brownian Motion and Stochastic Calculus* (Springer, New York, 1988).
5. D. Revuz and M. Yor, *Continuous Martingales and Brownian Motion* (Springer, Berlin, 1991).
6. P. E. Kloeden and E. Platen, *Numerical Solution of Stochastic Differential Equations* (Springer, Berlin, 1992).
7. D. Williams, *Probability with Martingales* (Cambridge University Press, Cambridge, 1991).
8. P. Mandel and T. Erneux, Laser Lorenz equations with a time-dependent parameter, *Phys. Rev. Lett.* **53**:1818–1820 (1984).
9. E. Benoît (Ed.), *Dynamic bifurcations* (Springer, Berlin, 1991).
10. V. I. Arnol'd (Ed.), *Dynamical Systems V* (Springer, Berlin, 1994).
11. C. W. Meyer, G. Ahlers, and D. S. Cannell, Stochastic influences on pattern formation in Rayleigh-Bénard convection: Ramping experiments, *Phys. Rev. A* **44**:2514–2537 (1991).
12. M. C. Cross and P. C. Hohenberg, Pattern formation outside of equilibrium, *Rev. Mod. Phys.* **92**:851–1089 (1993).
13. M. C. Torrent and M. San Miguel, Stochastic-dynamics characterization of delayed laser threshold instability with swept control parameter, *Phys. Rev. A* **38**:245–251 (1988).

14. N. G. Stocks, R. Mannella, and P. V. E. McClintock, Influence of random fluctuations on delayed bifurcations: The case of additive white noise, *Phys. Rev. A* **40**:5361 5369 (1989).
15. J. W. Swift, P. C. Hohenberg, and Guenter Ahlers, Stochastic Landau equation with time-dependent drift, *Phys. Rev. A* **43**:6572–6580 (1991).
16. G. D. Lythe and M. R. E. Proctor, Noise and slow-fast dynamics in a three-wave resonance problem, *Phys. Rev. E.* **47**:3122–3127 (1993).
17. G. Gaeta, Landau theory for phase transition with swept order parameter and noise: measurement of the transition delay, *Phys. Lett. A* **194**:419–423 (1994).
18. G. D. Lythe, Dynamics controlled by additive noise, *Nuovo Cimento D* **17**:855–861 (1995).
19. G. D. Lythe, in *Chaos and Nonlinear Mechanics*, T. Kapitaniak and J. Brindley (eds). *Nonlinear Science B* **7**:147–158 (1994).
20. G. D. Lythe, Domain formation in transitions with noise and a time-dependent bifurcation parameter, *Phys. Rev. E* **53**:R4271–R4274 (1996).
21. J. Guckenheimer and P. Holmes, *Nonlinear Oscillations, Dynamical Systems and Bifurcations of Vector Fields* (Springer, New York, 1987).
22. C. Meunier and A. D. Verga, Noise and Bifurcations, *J. Stat. Phys.* **50**:345–375 (1988).
23. P. Jung, G. Gray, R. Roy, and P. Mandel, Scaling Law for Dynamical Hysteresis, *Phys. Rev. Lett.* **65**:1873–1876 (1990).
24. H. C. Tuckwell, *Stochastic Processes in the Neurosciences* (SIAM, Philadelphia, 1989).
25. Z. F. Mainen and T. J. Seijnowski, Reliability of Spike Timing in Neocortical Neurons, *Science* **268**:1503–1506 (1995).
26. A. R. Bulsara *et al.*, Cooperative behaviour in periodically driven noisy integrate-fire models of neuronal networks, *Phys. Rev. E* **53**:3958–3969 (1996).
27. V. I. Kryukov, Wald's Identity and Random Walk Models for Neuron Firing, *Adv. Appl. Probab.* **8**:257–277 (1976).
28. J. R. Clay and N. S. Goel, Diffusion Models for Firing of a Neuron with varying Threshold, *J. Theor. Biol.* **39**:633–644 (1973).
29. J. R. Norris, L. C. G. Rogers, and D. Williams, Self-avoiding random walk: a Brownian-motion model with local time drift, *Prob. Th. Relat. Fields* **74**:271–287 (1987).
30. H. C. Tuckwell, *Elementary Applications of Probability Theory* (Chapman and Hall, London, 1995).
31. K. M. Jansons and L. C. G. Rogers, Probability and Dispersion Theory, *IMA J. Appl. Math.* **55**:149–162 (1995).
32. D. Dean and K. M. Jansons, Brownian Excursions on Combs, *J. Stat. Phys.* **70**:1313–1332 (1993).
33. A. Greuner, W. Strittmatter, and J. Honerkamp, Numerical Integration of Stochastic Differential Equations, *J. Stat. Phys.* **51**:95–108 (1988).